Aluminium phthalocyanine chloride thin films for temperature sensing*

Muhammad Tariq Saeed Chani[a)†], Abdullah M. Asiri[a)b)], Kh. S. Karimov[c)d)], Atif Khan Niaz[c)], Sher Bhadar Khan[a)b)], and Khalid. A. Alamry[b)]

[a)] *Center of Excellence for Advanced Materials Research, King Abdulaziz University, Jeddah* 21589, *Saudi Arabia*
[b)] *Department of Chemistry, Faculty of Science, King Abdulaziz University, Jeddah* 21589, *Saudi Arabia*
[c)] *GIK Institute of Engineering Sciences and Technology, Topi* 23640, *Pakistan*
[d)] *Physical Technical Institute, Aini St.* 299/1, *Dushanbe* 734063, *Tajikistan*

(Received 6 March 2013; revised manuscript received 17 May 2013)

This study presents the fabrication and temperature sensing properties of sensors based on aluminium phthalocyanine chloride (AlPcCl) thin films. To fabricate the sensors, 50-nm-thick electrodes with 50-μm gaps between them are deposited on glass substrates. AlPcCl thin films with thickness of 50–100 nm are deposited in the gap between electrodes by thermal evaporation. The resistance of the sensors decreases with increasing thickness and the annealing at 100 °C results in an increase in the initial resistance of sensors up to 24%. The sensing mechanism is based on the change in resistance with temperature. For temperature varying from 25 °C to 80 °C, the change in resistance is up to 60%. Simulation is carried out and results obtained coincide with experimental data with an error of ±1%.

Keywords: temperature sensor, thin films, annealing, aluminium phthalocyanine chloride

PACS: 81.05.Fb, 85.30.−z, 81.15.−z, 72.80.Le **DOI:** 10.1088/1674-1056/22/11/118101

1. Introduction

Temperature measurement is not only important for the comfort of human beings but also essential for other living organisms, agriculture, industrial processes, storage transportation, etc. Temperature sensors are normally categorized into contact and non-contact sensors. The former type includes resistance temperature detectors (RTDs) and thermocouples. The RTDs may also be classified into thermal sensitive resistors (thermistors) and resistance wire RTDs. For the fabrication of temperature sensors, the most commonly used sensing materials are platinum and gold, which are very expensive.[1,2] Cheap, low-density, flexible, and easy-to-fabricate materials have been used to replace expensive sensing materials. For this purpose, organic materials are considered to be very promising.[3–6] Resistance-temperature devices were found to be highly sensitive and accurate. For some cryogenic applications, carbon-based resistance-temperature sensors are currently being used.

The metal phthalocyanines (MPcs) are nontoxic p-type organic materials with good thermal and chemical stability. These materials are extremely attractive for use in optical and electronic devices. Currently, researchers are trying to explore the potentials of these materials for organic electronic devices like organic sensors, solar cells, FETs, OLEDs, etc.[7–13] The properties and the efficiency of the electronic devices are strongly dependent on the nature of the material and its processing, design, and fabrication technique.[14,15] The factors including film preparation technique, thickness and morphology of film, temperature of annealing, and sensing are very important for the performance of electronic devices.[16]

An organic semiconductor aluminium phthalocyanine chloride (AlPcCl) is a material with low molecular weight, low density (1.0 g/cm^3), and band-gap energy of 1.56 eV. As far as electronics applications are concerned the AlPcCl has been studied up to a limited extent for chemical and gas sensing applications and also for organic solar cells.[4,17] Recently, our group investigated AlPcCl films for humidity sensing applications and found it highly sensitive to humidity with short response and recovery time.[18] Thin film devices (surface type) were also fabricated for sensing application by Kato *et al*.[19] They studied the effect of ethanol vapor treatment on the current versus voltage characteristics of AlPcCl films. The ethanol vapor treated AlPcCl films showed significant change in conduction current as compared to as fabricated films. AlPcCl was investigated by Kim *et al* for solar cell application. They found an enhancement of efficiency of 1.8 times as compared to copper phthalocyanine based solar cells.[17] The photovoltaic devices based on AlPcCl (donor) and C_{60} (acceptor) are fabricated by Ballarotto *et al*.[20] The effect of interfacial layers (applied between ITO and AlPcCl) on open circuit voltage (V_{oc}) has been studied. The synthesis of AlPcCl and fabrication of sandwich-type devices (Au/AlPcCl/Au) has been carried out by Azimaraghi.[14] In his research he studied the electronic structure and conduction mechanism of AlPcCl thin

*Project supported by the Center of Excellence for Advanced Materials Research (CEAMR), King Abdulaziz University, Jeddah (Grant No. CEAMR-434-03).
†Corresponding author. E-mail: tariq_chani@yahoo.com; tariqchani1@gmail.com
© 2013 Chinese Physical Society and IOP Publishing Ltd

films under different operating conditions. It is also reported that the capacitance of Au/AlPcCl/Au devices increased with increase in temperature.

Based on our previous efforts in the fabrication of various types of sensors[21–25] and the fact that AlPcCl has a sufficiently large energy gap, here we report the fabrication and investigation of resistance-temperature sensors based on AlPcCl thin films.

2. Experimental details

AlPcCl has been used for the fabrication of samples and is commercially available from Sigma Aldrich. AlPcCl has a chemical formula C_{32} $H_{16}AlClN_8$, its molecular weight is 574.96, and its molecular structure is shown in Fig. 1(a). To fabricate the sensors, aluminium electrodes are deposited on a glass substrate by using an EDWARD 306 vacuum thermal evaporator. The 50-nm-thick electrodes have an area of 12×25 mm^2 and there is a gap of 50 μm between two electrodes, where AlPcCl films of 50, 70, and 100 nm thick are also deposited by using a thermal evaporator. The deposition is carried out under vacuum of 1.6×10^{-5} mbar and the rate of deposition is maintained at 0.1–0.2 nm/s. The scheme of fabrication process and the schematic diagram of the sensor are shown in Figs. 1(b) and 1(c), respectively. The fabricated sensors were also annealed at 100 °C for one hour.

The resistance of the sensors at a frequency of 1000 Hz and 10000 Hz is calculated with measured values of capacitance (C) and dissipation (D) by using the following expression:[26]

$$R = 1/(2\pi fCD). \quad (1)$$

An Agilent U1732A LCR meter is used for the measurements of capacitance and dissipation. To confirm the repeatability of the sensors, testing is carried out three times.

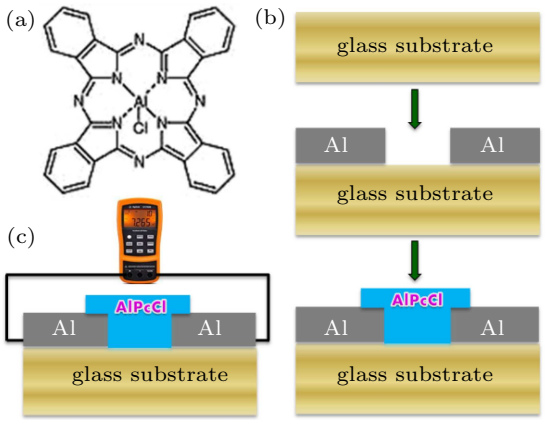


Fig. 1. (color online) (a) Molecular structure of AlPcCl, (b) scheme of the fabrication process, and (c) schematic diagram of Al–AlPcCl–Al sensor.

3. Results and discussion

The resistance–temperature relationships of as-fabricated 50-nm-thick and 100-nm-thick AlPcCl film sensors at a frequency of 1 kHz are shown in Figs. 2(a) and 2(b), respectively. It is evident from the figures that the change in temperature from 25 °C to 80 °C causes 70% and 88% nonlinear decrease in the resistance of the sensors with 50-nm-thick and 100-nm-thick film, correspondingly. It is also clear that resistance decreases with increase in thickness. This behavior is also reported for copper phthalocyanine films in Refs. [27] and [28]. The resistance–temperature relationship of 70-nm-thick film is similar to that of 50-nm-thick film and its initial resistance is 362 MΩ. The smaller resistance of thick films is attributed to their increased crystallite size as compared to thin films.

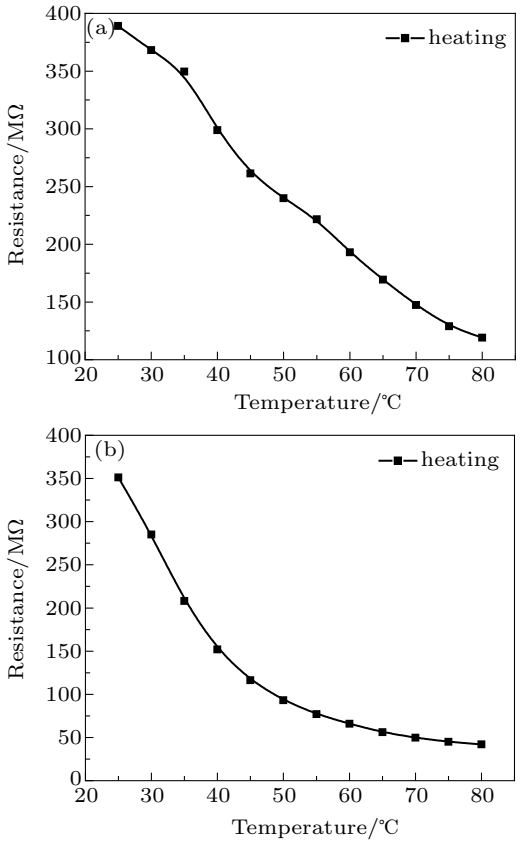


Fig. 2. Resistance-temperature relationship of sensors at a frequency of 1000 Hz. Sensor with (a) 50-nm-thick and (b) 100-nm-thick AlPcCl film (as fabricated).

It can be seen that the tendency shown in Fig. 2(a) is slightly different from that in Fig. 2(b). The possible reason for this difference may be the following: usually the surface structure and accordingly the properties of the solids differ from the bulk structure and properties. Therefore, this tendency difference may be the result of effects of the surface and bulk resistance behavior of the samples at various temperatures. Usually, in thin films (50 nm) the contribution of surface structure and accordingly the resistance is larger as com-

pared to thick films (100 nm), which may result in difference in resistance–temperature behavior.

Post deposition annealing proves to be very promising for the long-term stability of sensors by re-organization of structure.[16] To obtain the stabilized response, annealing of samples is also carried out. Figures 3(a) and 3(b) show the normalized resistance–temperature relationship of sensors in an annealed condition at 1000 Hz. In this condition, the response of the sensors is more linear than sensors in as-fabricated condition. After annealing, the initial resistance of the sensors increases by 14% and 24%, and it may be attributed to the increase in the porosity of films as a result of annealing.[18] Figures 4(a) and 4(b) show the SEM image of AlPcCl films before and after annealing respectively. It is evident from the surface morphology that the porosity increases as a result of annealing.

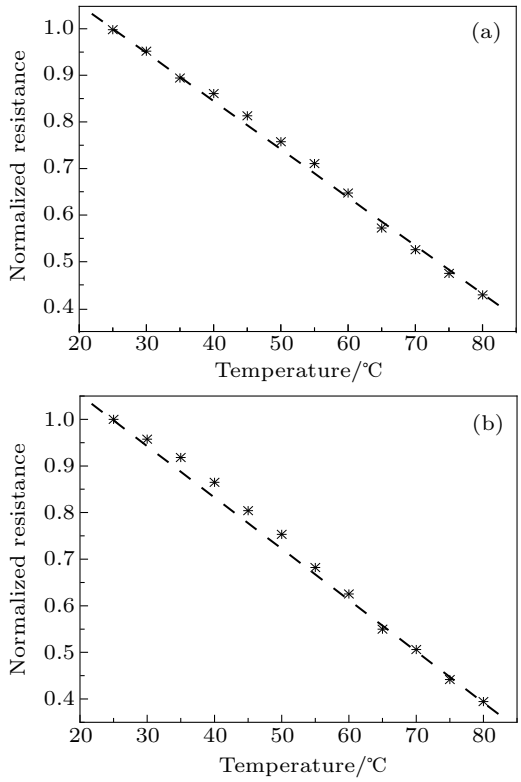


Fig. 3. Normalized resistance-temperature relationship of sensors at a frequency of 1000 Hz Sensor with (a) 50-nm-thick and (b) 100-nm-thick AlPcCl film (annealed).

Table 1. Effect of film thickness and frequency on the resistance of sensors.

Film thickness/nm	Frequency/kHz	Change in resistance/%	
		As-fabricated	Annealed
50	1	70.0	58.0
	10	28.0	15.2
100	1	88.0	60.7
	10	34.8	14.2

The decrease in resistance as a result of increase in temperature from 25 °C to 80 °C is up to 60% for both sensors. As shown in Figs. 5(a) and 5(b), the sensors exhibit small hysteresis (±2.5%), that may be attributed to annealing. The small hysteresis is essential quality of the best sensors, which may not be found commonly in the organic materials based sensors. It is also observed that the resistance decreases with increase in frequency, and the change in resistance at higher frequency with temperature is smaller than resistance change at lower frequency. The effect of film thickness and frequency on the resistance of the sensors is shown in Table 1.

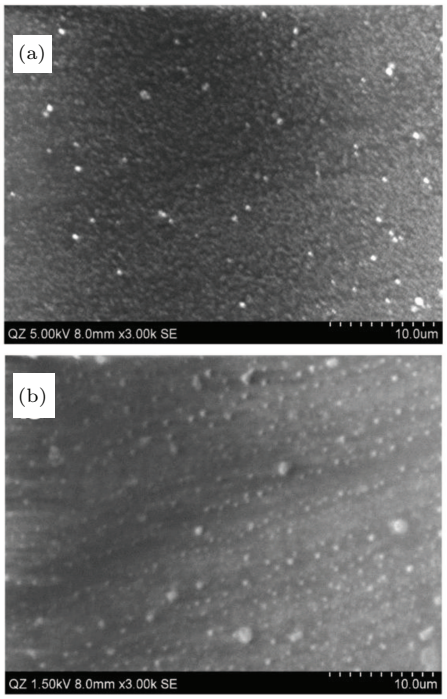


Fig. 4. Morphology of AlPcCl film (a) before and (b) after annealing.

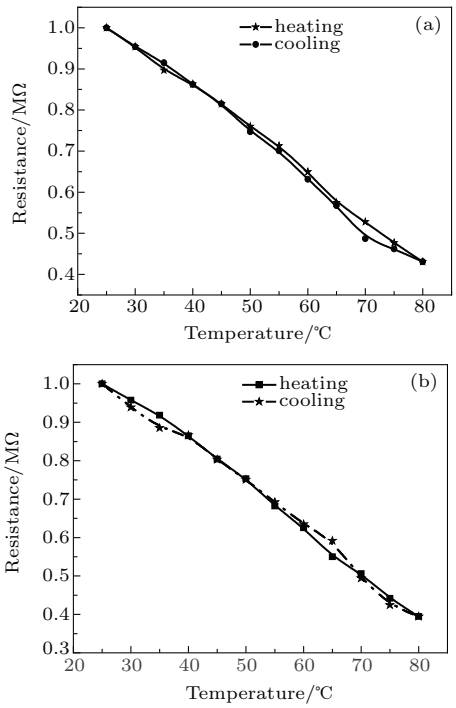


Fig. 5. Hysteresis of the sensors at a frequency of 1000 Hz. Sensor with (a) 50-nm-thick and (b) 100-nm-thick AlPcCl film (annealed).

The resistance (R) of the sensors can also be determined by the following expression:[29]

$$R = \frac{d\rho}{A} = \frac{d}{\sigma A}, \tag{2}$$

where d is the inter-electrode distance, ρ is resistivity, σ is conductivity, and A is the cross-sectional area of the AlPcCl film. The increase in the conductivity of the sensors with increase in temperature is attributed to the increase in the density of charge carriers as a result of temperature elevation.[30] The resistance temperature coefficient of the sensors may be calculated by

$$S = \Delta R/(R_o \Delta T), \tag{3}$$

where S is the resistance temperature coefficient, R_o is the initial resistance, ΔR is the change in resistance, and ΔT is the change in temperature. The value of S for the data shown in Figs. 5(a) and 5(b) is found to be $-0.99\%^{\circ}\mathrm{C}^{-1}$ and $-1.01\%^{\circ}\mathrm{C}^{-1}$ respectively, which are on average $-1.37\%^{\circ}\mathrm{C}^{-1}$ and $-2.7\%^{\circ}\mathrm{C}^{-1}$ in as-fabricated conditions. The results indicate that sensor with 50-nm-thick organic films has more stable resistance temperature coefficient than 100-nm-thick film in both conditions.

The conduction mechanism in aluminiun phthalocyanine films may also be considered as transitions between spatially separated molecules or sites, which may be credited to the percolation theory.[31,32] Considering the percolation theory, following relationship can be used for the calculation of effective conductivity σ,

$$\sigma = \frac{1}{LZ}. \tag{4}$$

Here, L represents the characteristic length, which depends on the concentration of sites, while Z is the resistance of a path with the lowest average resistance. The increase in temperature causes charge carriers, which results in reduction of Z.

The simulation of resistance temperature relationship has been carried out for both of the sensors. The following mathematical function is used for the simulation in its modified form:[33]

$$f(x) = \mathrm{e}^{-x}. \tag{5}$$

The modified form of the function used for the simulation of sensor with 50-nm-thick AlPcCl film is given by

$$R/R_{\mathrm{o}} = \mathrm{e}^{-\Delta T(2T/(T+T_{\mathrm{m}}))K_1}. \tag{6}$$

While for the simulation of resistancetemperature relationship of sensor with 100-nm-thick organic film modified function is given by

$$R/R_{\mathrm{o}} = \mathrm{e}^{-\Delta T(T/T_{\mathrm{m}})K_2}. \tag{7}$$

In Eqs. (6) and (7), R_0 and R are the sample's initial resistance and the resistance at elevated temperatures (T), respectively, and T_{m} is the maximum temperature, while K_1 and K_2 are the resistance–temperature factors. The value of resistance–temperature factor is calculated from the experimental data given in Figs. 5(a) and 5(b). The calculated value of K_1 and K_2 is 1.53% $^{\circ}\mathrm{C}^{-1}$ and 1.67% $^{\circ}\mathrm{C}^{-1}$ respectively. The comparison of simulated and experimental (using Eqs. (6) and (7)) results is shown in Figs. 6(a) and 6(b). It can be seen that simulated results coincide with experimental results with an error of $\pm 1\%$ and $\pm 2\%$ respectively for 50-nm-thick and 100-nm-thick AlPcCl film.

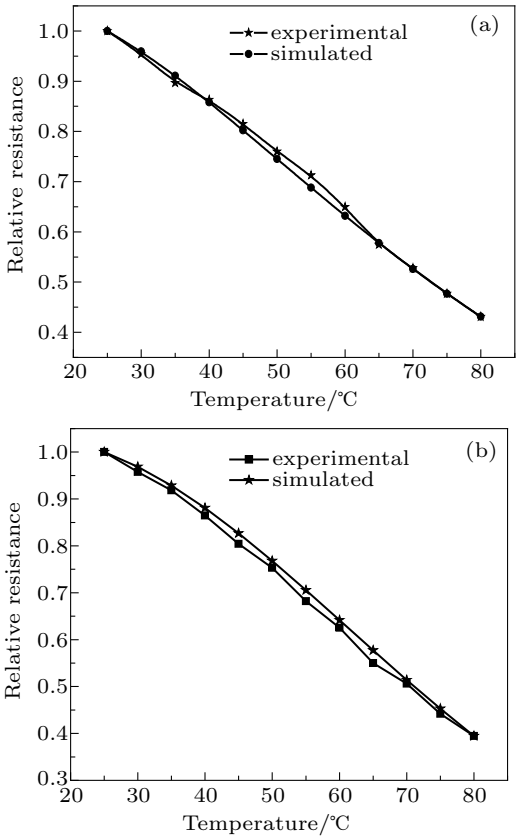


Fig. 6. Comparison of experimental and simulated results for sensor with (a) 50-nm-thick and (b) 100-nm-thick AlPcCl film.

4. Conclusions

The temperature sensing properties of sensors (resistive type) based on AlPcCl thin films deposited by vacuum thermal evaporation have been investigated. The sensing mechanism is based on the variation of resistance with change in temperature. Sensors show higher sensitivity to temperature, which is credited to the generation of charge carriers under the effect of elevating temperature. It is found that annealing results in 14%–24% increase in the initial resistance of the sensors. The resistance–temperature behavior is quasi-linear in the temperature range of 25–80°C, and the sensors show small hysteresis ($\pm 2.5\%$). These changes are attributed to the porous formation of the AlPcCl film. The resistance–temperature sensors may be used as the instruments for environmental monitoring and assessment of temperature.

References

[1] Lee C Y, Wu G W and Hsieh W J 2008 *Sensor. Actuat. A* **147** 173
[2] Park J J and Taya M 2005 *J. Electron. Packaging* **127** 286
[3] Cho S, Piper L, DeMasi A, Preston A, Smith K, Chauhan K, Sullivan P, Hatton R and Jones T 2010 *J. Phys. Chem. C* **114** 1928
[4] Drechsel J, Mannig B, Gebeyehu D, Pfeiffer M, Leo K and Hoppe H 2004 *Org. Electron.* **5** 175
[5] Reboun J, Hamacek A, Dzugan T and Kroupa M 2010 33*rd International Spring Seminar on Electronics Technology (ISSE)*, 12–16 May, 2010 Warsaw, Poland p. 40
[6] Mathew S, Kumar C S and Menon C S 2010 *OAM-RC* **4** 63
[7] Hooper P D 1996 *Int. J. Electron.* **81** 371
[8] Lohani J, Gaur M, Kumar U, Balakrishnan V R, Harsh and Eswaran S V 2010 *Chin. Phys. Lett.* **27** 048102
[9] Huang Z, Su W and Zeng X T 2007 *SIMTech. Technol. Rep.* **8** 182
[10] Feng P, Rui X Q, Zhen L H, Bo H W and Hang D Y 2011 *Chin. Phys. Lett.* **28** 078504
[11] Larbi A, Djedou B, Bennacer L and Salah M B 2009 *Int. J. Smart Sens. Intell. Syst.* **2** 448
[12] Zheng C, Bo D Z, Yang Z M, Yue L Z, Liang D H, Ye Z, Hong Y Y and Chao L J 2012 *Chin. Phys. Lett.* **29** 078801
[13] Fang Z Q, Cheng C H, Yu K Q, Ye S K, He W, Cheng X D, Guo Z Q, Sheng R S, Wang X and Du X G 2008 *Chin. Phys. Lett.* **25** 2261
[14] Azimaraghi M E 2007 *Ind. J. Pure Appl. Phys.* **45** 40
[15] Papageorgiou N, Salomon E, Angot T, Layet J M, Giovanelli L and Lay G L 2004 *Prog. Surf. Sci.* **77** 139
[16] Lee Y L, Hsiao C Y and Hsiao R H 2004 *Thin Solid Films* **468** 280
[17] Kim D Y, So F and Gao Y 2009 *Sol. Energy Mater. Sol. Cells* **93** 1688
[18] Chani M T S, Karimov K S, Khalid F A, Raza K, Farooq M U and Zafar Q 2012 *Physica E* **45** 77
[19] Kato K, Saito Y, Ohdaira Y, Shinbo K and Kaneko F 2006 *Thin Solid Films* **499** 174
[20] Ballarotto M, Herman W N and Romero D B 2011 *J. Photon. Energy* **1** 011102
[21] Karimov K S, Chani M T S, Khalid F A and Khan A 2012 *Physica E* **44** 778
[22] Chani M T S, Karimov K S, Khalid F A, Abbas S Z and Bhatty M B 2013 *Chin. Phys. B* **22** 010701
[23] Karimov K S, Chani M T S, Khalid F A and Moiz S A 2011 *Chin. Phys. B* **20** 040601
[24] Karimov K S, Chani M T S and Khalid F A 2011 *Physica E* **43** 1701
[25] Karimov K S, Chani M T S, Khalid F A, Khan A and Khan R 2012 *Chin. Phys. B* **21** 016102
[26] Irwin J D 1999 *Basic Engineering Circuit Analysis* (6th Edn.) (New York: John Wiley & Sons)
[27] Nahass M M E, Bahabri F S, Ghamdi A A A and Harbi S R A 2002 *Egypt. J. Sol.* **25** 307
[28] Hassan A K, Gould R D and Ray A K 2006 *Phys. Stat. Sol. (a)* **158** K23
[29] Omar M A 2002 *Elementary Solid State Physics: Principles and Applications* (Singapore: Pearson Education Pt. Ltd.)
[30] Neamen D A 1992 *Semiconductor Physics and Devices: Basic Principles* (Boston: Richard D. Irwin Inc.)
[31] Brabec C J, Dyakonov V, Parisi J and Sariciftci N S 2003 *Organic Photovoltaics: Concepts and Realization* (Berlin: Springer-Verlag)
[32] Bottger H and Bryksin V V 1985 *Hopping Conductions in Solids* (Berlin: VCH Publishers Akademie-Verlag)
[33] Croft A, Davison R and Hargreaves M 1993 *Engineering Mathematics: A Modern Foundation for Electronic, Electrical and Control Engineers* (Great Britain: Addison-Wesley Publishing Company)